*International Journal of Environment, Agriculture and Biotechnology*
*Vol-9, Issue-6; Nov-Dec, 2024*
*Peer-Reviewed International Journal*
*Journal Home Page Available:*https://ijeab.com/
*Journal DOI:*10.22161/ijeab

# Green Synthesis and DFT study of Nickel Zinc Ferrite Nanoparticles: A Highly Sensitive Room Temperature VOC Sensing Material

Chandra Mukherjee[1*], Subhankar Choudhury[2], Nabajyoti Baildya[3], Narendra Nath Ghosh[4], Debabrata Misra[5], J. Das[6]

[1]The Neotia University, D.H.Road, Kolkata- 743368, India.
[2]Department of Chemistry, Malda College, Malda, 732101, India.
[3]Department of Chemistry, University of Kalyani, Kalyani 741235, India.
[4]Department of Chemistry, University of Gour Banga, Mokdumpur, Malda 732103, India.
[5]Department of Botany, University of Gour Banga, Mokdumpur, Malda 732103, India.
[6]The Department of Physics, Jadavpur University, Kolkata-700032, India.
*Corresponding author: chandra.mukherjee@tnu.in

Received: 30 Oct 2024; Received in revised form: 01 Dec 2024; Accepted: 08 Dec 2024; Available online: 14 Dec 2024


***Abstract*****—** *In present communication, nanocrystalline nickel zinc ferrite (NZF) has been prepared by spin controlled coprecipitation method in varied proportions to study the alcohol (primary alcohols viz. ethanol, propanol and butanol) sensing behaviour at room temperature. Nanocrystalline nickel zinc ferrite (NZF)* $Ni_{1-x}Zn_xFe_2O_4$ *(where x = 0.3, 0.5 and 0.7) are subjected to the structural and surface morphological characterizations, porosity and surface activity through Powder X-ray Diffraction (PXRD) and Field Emission Scanning Electron Microscopy (FESEM). The variations in electrical resistance of* $Ni_{0.7}Zn_{0.3}Fe_2O_4$ *(NZF1),* $Ni_{0.5}Zn_{0.5}Fe_2O_4$ *(NZF2) and* $Ni_{0.3}Zn_{0.7}Fe_2O_4$ *(NZF3) are measured with the exposure of 500 ppm ethanol, propanol and butanol vapours as a time function at room temperature. 89% sensitivity is detected by NFZ1 for 500 ppm of ethanol vapour. The sensing response followed the order of ethanol > propanol > butanol for all the three samples. The increasing trend of VOC (volatile organic substance) sensing properties by NZFs has been verified through extensive DFT (density functional theory) analysis by adopting PAW (projector augmented wave) technique. DFT calculation supports the pulling effect of Ni atoms in NZF nanoparticles which consequently increases the sensing properties of the NZFs. ELF (Electron localization function) study also supports the accelerated adsorption capacity of nickel doped nanoferrites.*

***Keywords*****— Coprecipitation, DFT study, Nanostructural analysis, NiZn ferrites, room temperature VOC sensor.**

## I. INTRODUCTION

Under volatile organic compounds (VOCs), primary aliphatic alcohols like ethanol, propanol and butanol are the most common and widely used harmful toxicants. Reliable detection of hazardous, harmful and toxic vapours is now become a major issue in the field of environmental protection worldwide. For continuous measurement of these volatile organic substances, inexpensive, sensitive, easy to operate and stable sensor sdevices are required. Nanostructured materials including metal oxides, carbon nanotubes, graphene and conducting polymer, nanocarbon composites are being vigorously explored in sensing of various organic vapours [1-6]. In spite of poor selectivity and high working temperature, particularly the nanostructured metal oxides like $SnO_2$, ZnO, $Fe_2O_3$ and $WO_3$ have been widely used in alcohol vapour sensing [7-11]. Spinel type metal ferrites with formula $MFe_2O_4$ is proven to be a reliable sensor material for room

temperature sensing of both oxidizing and reducing vapours overcoming the high temperature and selectivity constrain [12, 13]. Among different ferrite materials, n-type zinc ferrite semiconductor is a widely adopted for the detection of ethanol, acetone, hydrogen and $H_2S$ [14-18]. Due to thermal stability, low cost and moreover simple preparation of spinel ferrites, it becomes a high priority commercially viable electronic material in recent days. Nanostructured mixed ferrites offer a strong surface reactivity towards gases and organic vapours due to their small grain size, high density of grain boundaries and interfaces. Hence are expected to be more sensitive, selective and long-term stable sensor provisions [19-20].

The present work reveals a comparative study of the response behaviour of prepared nanocrystalline nickelzinc ferrite (NZFs) toward the primary aliphatic alcohols like, ethanol, propanol and butanol at ambient temperature. Ethanol, propanol and butanol have been widely used in various manufacturing units, industries and scientific laboratories. Ethanol as a hypnotic solvent is widely applied in the manufacture of wine, medical processes, food industries and biomarker as well [21]. Propanol is used as a cleansing solvent for oil. Long term exposure to propanol can lead to skin irritation and other health complications [22]. Butanol is widely used as dye diluent in textile and chemical units. It also finds its application in the manufacture of biofuels now-a-days. But its toxicity ranges from eye and skin irritation to the central nervous system damage on prolonged exposure.

Hence there is a great search for the suitable, selective and economically viable sensors to monitor VOCs.

## II. MATERIALS AND METHODS

### 2.1. Preparation

$Ni_{0.7}Zn_{0.3}Fe_2O_4$ (NZF1), $Ni_{0.5}Zn_{0.5}Fe_2O_4$ (NZF2) and $Ni_{0.3}Zn_{0.7}Fe_2O_4$ (NZF3) have been successfully prepared by coprecipitation method in varied proportion. Detailed techniques for nanoferrites synthesis are described in the previous article [23]. Post annealed samples are regrind and desiccated for further characterization and analysis.

### 2.2. Structural characterization

X-ray powder diffraction has been recorded using a Bruker´D8 Advance´ Diffractometer (funded by UGC-DRS (SAP-II) DST (FIST-II), at Jadavpur University), equipped with a Globel mirror using Cu Kα (λ = 1.54184A°) radiation. The generator setting was maintained at 40kV and 40mA.The diffraction patterns has been recorded at ambient temperature with a counting time of 2 s/step over a range of $2\theta=20^0$- $90^0$.

The interplane spacing $d$ has been calculated by using Bragg's Law equation,

$$d = \frac{\lambda}{2Sin\theta} \quad (1)$$

where $\Theta$ is Bragg's diffraction angle calculated by equating $2\,\Theta$ with the peak value from XRD pattern, λ is wavelength of Cu Kα (λ = 1.54184A°) radiation.

The following equation has been utilised to calculate the lattice constant $a$ for the NZF samples from the diffraction planes.

$$a = d\sqrt{(h^2 + k^2 + l^2)} \quad (2)$$

where $d$ is the interplane spacing, $h, k, and\ l$ are the Miller indices of the crystal planes after fitting, the 100 line (311 plane) of the XRD pattern of the prepared NZFs [24].

The theoretical density of the samples is determined from XRD data by:

$$\rho_x = \frac{8M}{Na^3} \quad (3)$$

Where $\rho_x$the density is calculated from XRD data, $M$ is the molecular weight, $N$ is the Avogadro's number, and $a$ is the lattice constant of the cubic unit cell [25].

The experimental density $\rho_m$ of the annealed samples is determined by considering the cylindrical shape of the pellet by the following equation:

$$\rho_m = \frac{m}{\pi r^2 h} \quad (4)$$

Where $m$ is the mass, $r$ is the radius and $h$ is the thickness of the pellet [26].

Porosity $P$ of the pellet is determined through the relation:

$$P = \frac{\rho_x - \rho_m}{\rho_x} \times 100 \quad (5)$$

Where $\rho_m$ and $\rho_x$ are the experimental and theoretical densities respectively [27].

Investigation of surface morphology of the prepared NZFs have been carried out by the FESEM facility (FEI, INSPECT F 50) equipped with an energy dispersive x-ray spectrometer system, (configuration no. QUO-35357-0614 funded by FIST-II, DST, Government of India), at the Physics Department, Jadavpur University.

### 2.3. Measurements

The palletization technique and criteria of the NZF samples is described in former article [23]. Highly pure silver paste electrode is used to coat the surface of the pellets. The VOC sensing behaviours of NZF1, NZF2 and NZF3 is measured using a static flow vapour sensing set up, developed in our laboratory Fig 1. Vapour sensing measurements are performed in a closed test chamber at a static atmosphere in the ambient temperature. In order to improve the

stability of vapour sensor the sensing element is kept in the sensing chamber for more than 12 hours before testing.

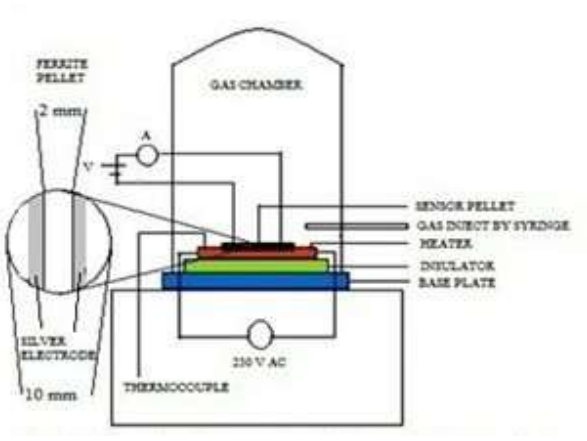


*Fig 1: Schematic diagram of static flow vapour sensing*

## III. RESULTS AND DISCUSSION

### 3.1. Material characterizations

XRD pattern of all NZF samples, annealed at 1200̊ C is presented in Fig. 2 below. Prepared NZFs are found to form cubic spinel type structure without any peaks from other phases. The sharp diffraction peaks indicate a high degree of crystallization for the obtained metal ferrite compounds.

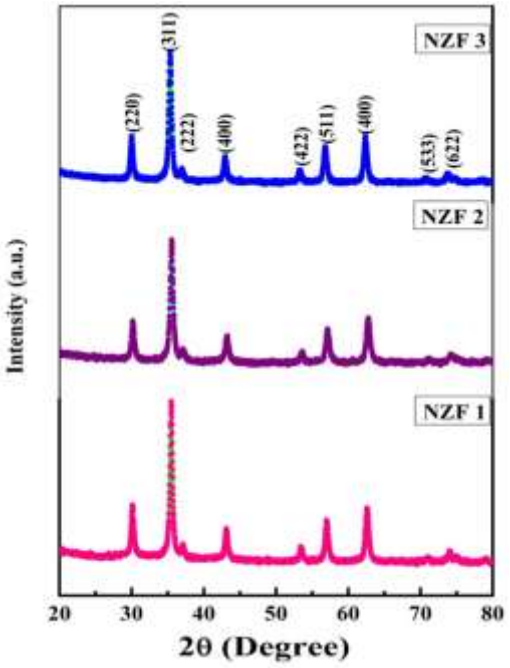


*Fig.2. PXRD pattern of NZF1, NZF2 and NZF3.*

The sensing response is calculated using the given formula.

$$S\% = \left(\frac{\Delta R}{R_{air}}\right)\times 100$$

$$\text{or } S\% = \left(\frac{|R_{air} - R_{gas}|}{R_{air}}\right)\times 100 \quad (6)$$

Where $R_{air}$ and $R_{gas}$ are resistance in the air and the presence of test vapours respectively and ΔR is the resistance variation. The resistance variation of NZF samples is recorded at room temperature with different alcohol vapours. Heater with thermocouple is used here for resetting of the sensor pellet to perform repetitive experiments. This is aimed to further study by optimizing the temperature for different VOCs with varied concentrations. Some crystalline properties of NZFs are compared and shown in Table 1. The calculated lattice constant 'a' is seen to increase with increase in zinc content. The variation in lattice constant can be explained on the basis of the ionic radii of $Zn^{2+}$ (0.82 Å) ions is higher than that of $Ni^{2+}$ (0.78 Å) [28, 29]. Fig.3a. 3b and 3c present the FESEM micrographs for the prepared samples which show microstructures with nanosized grains. The low measured density with open porosity > 60%, thus satisfying the requirements for materials to be used as organic vapour sensors. Presence of both nanostructured grain size and porosity, increases the specific surface area of the prepared samples and make it suitable material for vapour sensing applications [30].

*Table 1. Properties of prepared NZF sensors*

| Composition | $a$ (Å) | $\rho_x$(g/cc) | $\rho_m$(g/cc) | $P$(%) |
|---|---|---|---|---|
| $Ni_{0.7}Zn_{0.3}Fe_2O_4$ | 8.338001 | 5.41645 | 1.99096 | 64.16546 |
| $Ni_{0.5}Zn_{0.5}Fe_2O_4$ | 8.386085 | 5.35393 | 1.99137 | 62.80534 |
| $Ni_{0.3}Zn_{0.7}Fe_2O_4$ | 8.434177 | 5.29248 | 2.01233 | 61.97756 |

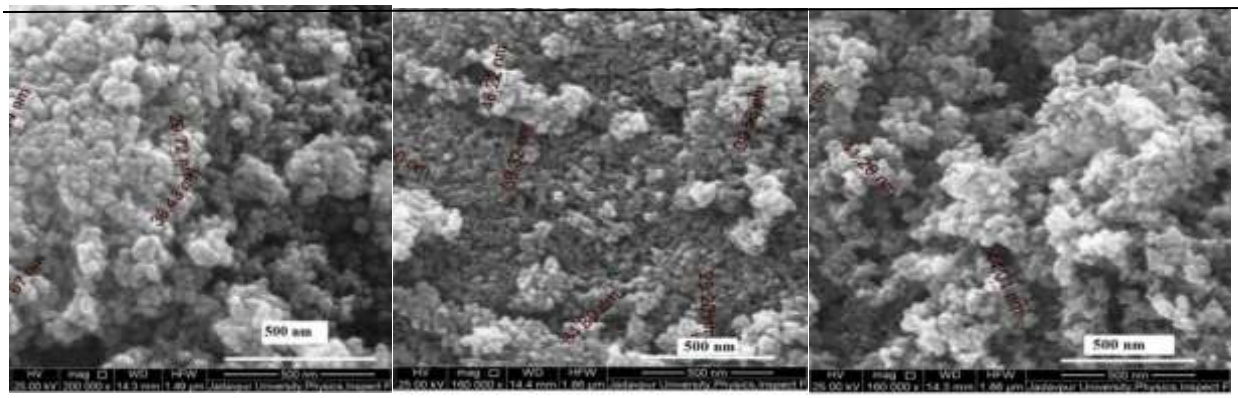


*Fig. 3a.* *Fig. 3b.* *Fig. 3c.*

*Fig. 3a. FESEM micrographs of NZF1, Fig. 3b. FESEM micrographs of NZF2, Fig.3c. FESEM micrographs of NZF3*

3.2. Alcohol sensing characteristics

3.2.1 Transient response study

Initially, the behavioral pattern of the vapour sensing by NZF pellets for different alcohol vapours are studied in the ambient temperature. The transient response of NZF1, NZF2 and NZF3 towards the vaopurs of 500 ppm ethanol, propanol and butanol with respect to time are shown in Fig. 4a, 4b and 4c respectively.

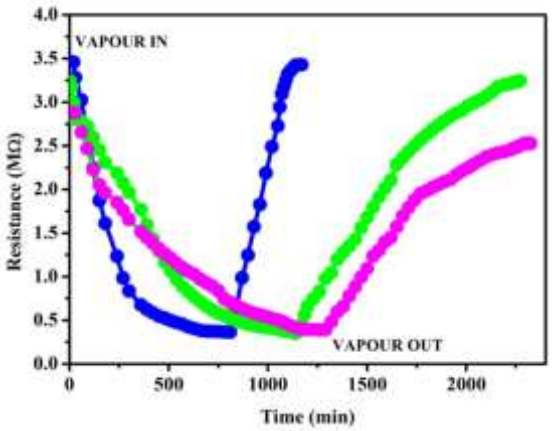


*Fig. 4a. Transient response of NZF1 for 500 ppm ethanol (blue), propanol (green) and butanol (pink) at room temperature.*

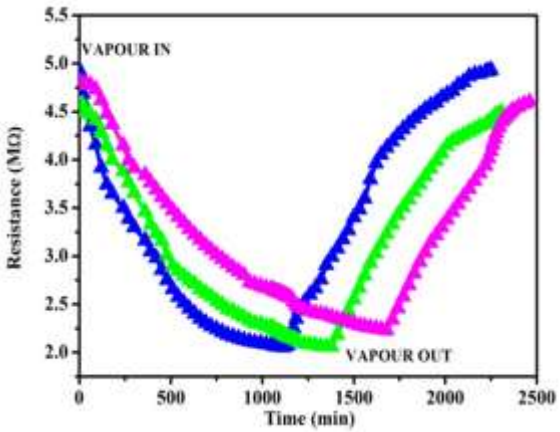


*Fig. 4b. Transient response of NZF2 for 500 ppm ethanol (blue), propanol (green) and butanol (pink) at room temperature.*

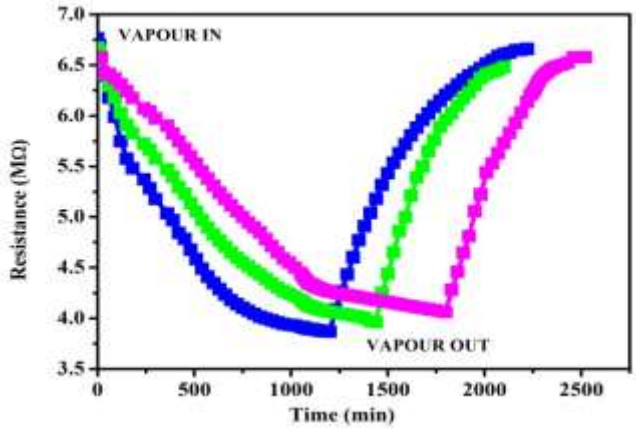


*Fig. 4c. Transient response of NZF3 for 500 ppm ethanol (blue), propanol (green) and butanol (pink) at room temperature.*

The electrical resistance by the sensor pallet is measured in presence of air before introducing any test vapour in the dome chamber. A quantity of 10 ml of test vapour is inserted in the chamber every time. As soon as the alcohol vapours are inserted, the NZF pellets exhibits lowering of the resistance responses and thus an increasing vapour sensing response is observed in all cases. After a steady response, alcohol vapours are removed from the closed dome by opening the lid and the response pattern is recorded again. The observations show a pretty stable and highly reproducible sensor responses by the samples even at room temperature.

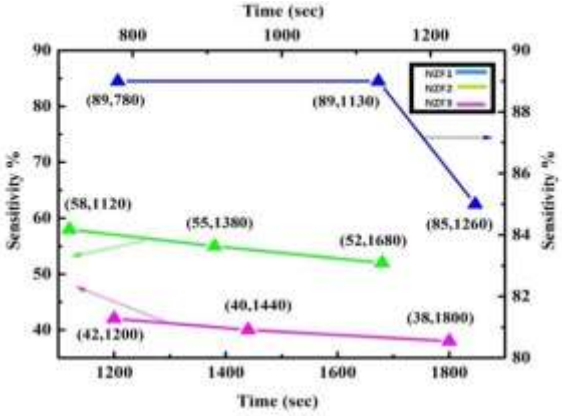


Fig. 5: Sensitivity response of NZF sensors with the response time.
NZF1 (blue): ethanol (89,780), propanol (89, 1130) and butanol (85, 1260)
NZF2 (green): ethanol (58, 1120), propanol (55, 1380) and butanol (52, 1680)
NZF3 (pink): ethanol (42, 1200), propanol (40, 1440) and butanol (38, 1800)

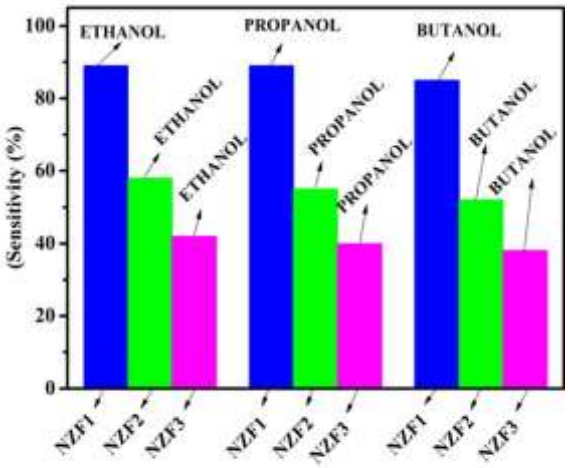


Fig. 6: Selective sensitivity of NZF1 (blue), NZF2 (green) and NZF3 (pink) towards 500 ppm ethanol, propanol and butanol at room temperature.

1.2.2. Sensitivity study

Fig.5 shows the sensitivity response of NZF1, NZF2 and NZF3 towards 500 ppm of ethanol, propanol and butanol vapours in accordance with the response time in the ambient temperature. The response and recovery time of the NZF nano samples towards different alcohol vapours are estimated from the respective resistance variation data. From the comparative study, the sensitivity is found to follow an order of NZF1 > NZF2 > NZF3 with average sensitivity value of 88%, 55% and 40% respectively towards alcohol vapour in the ambient temperature is summarized in Table 2. It took several minutes to recover the original resistance after removal of test vapours from the closed chamber. A long time recovery observed at room temperature is due to the agglomerated nature of the sensing element revealed by FESEM microstructure. When the NZF pellet is exposed to analyte vapours it goes deeper into the pellet and it comes out slowly at room temperature which results in a longer recovery time [31]. The stability data of the three alcohol sensors are obtained

under similar conditions at room temperature over a period of 30 days to confirm the reliability of the measurements.

1.2.3. Selectivity study

Selective detection of VOC is a big challenge for any commercial sensor. It is seen that, NZF1 is more selective towards alcohol vapour than NZF2 and NZF3 at ambient temperature. The selectivity study of the annealed NZF pellets has been carried out repeatedly through the exposure of 500 ppm of ethanol, propanol and butanol maintaining the similar ambient condition every time which has been clearly revealed from Fig.6.

*Table 2. Comparison of ethanol, propanol and butanol sensitivity characteristics of NZF sensors at room temperature.*

| Type of Sensing Materials | Test vapours | Concentration (ppm) | Maximum response (%) | Response time(min) | Recovery time(min) |
|---|---|---|---|---|---|
| NZF1 | Ethanol | 500 | 89 | 13 | 05 |
| | Propanol | 500 | 89 | 18 | 16 |
| | Butanol | 500 | 85 | 21 | 18 |
| NZF2 | Ethanol | 500 | 58 | 18 | 15 |
| | Propanol | 500 | 55 | 23 | 16 |
| | Butanol | 500 | 52 | 28 | 18 |
| NZF3 | Ethanol | 500 | 42 | 20 | 13 |
| | Propanol | 500 | 40 | 24 | 14 |
| | Butanol | 500 | 38 | 30 | 15 |

1.2.4. Sensing mechanism

It is observed that the resistance of the sensing element decreases when exposed to reducing vapours like ethanol, propanol and butanol which suggest that NZF sensors behave as n-type semiconductor. The vapour sensing mechanism of the metal ferrite is a surface controlled phenomenon that is based on the surface area of the pellet sensor at which the vapour molecules adsorb and react with pre-adsorbed oxygen molecules. As the prepared metal ferrites are highly porous, the oxygen chemisorptions centers like oxygen vacancies, localized donor and accepter states are formed on the surface during synthesis. These centers are filled by adsorption of oxygen molecules from air. After some time, equilibrium state is achieved between oxygen of metal ferrite and atmospheric oxygen. At room temperature, it took some time to give a stabilized resistance which is known as resistance of air ($R_a$). The ferrite interacts with oxygen by trapping the electrons from the conduction band to adsorbed oxygen atom, resulting in the formation of ionic species such as $O_2^-$ , $O^{2-}$ and $O^-$. The transferring of electrons from conduction band of the sample ferrite to adsorbed oxygen atoms may occur through the following reactions [32, 33].

$$O_2(air) \leftrightarrow O_2(ads)$$

$$O_2(ads) + e \leftrightarrow O_2^-(ads)$$

$$O_2^-(ads) + e^- \leftrightarrow 2O^-(ads)$$

$$O_2(ads) + 2e \leftrightarrow O^{2-}(ads)$$

The dropping of the electrical resistance occurs due to the release of more and more electrons back into the conduction band of ferrite as a result of the surface interaction between alcohol vapours attached with ferrites and the surface adsorbed oxygen. The reaction between $ROH$ vapours and adsorbed oxygen ions can take place as;

Alcohol: $ROH_{vap} + O_{ad}^{2-} \rightarrow RO_{ad}^- + OH_{ad}^-$

$$RO_{ad}^- \rightarrow R_2O + O_{ad}^- + e^-$$

$$ROH_{vap} + O_{ad}^{2-} + \text{hole} \rightarrow CO_2 + H_2O + v_0^-$$

(Where $v_0^-$ is a doubly charged oxygen vacancy)

These reactions divert electrons back to the conduction band of the sensing ferrites leading to an increase in electron concentration and a decrease in resistance [34]. After input of test vapours, due to liberation of electrons, the resistance of sensing ferrites decreases drastically at beginning because of rapid adsorption and afterwards it decreases slowly and finally become saturated. Because $OH^-$ group is present on surface of ferrite nanostructure, which can form hydrogen bond with isolated electron pair at oxygen atom. Hence, the physical adsorption to alcohol vapour of ferrite is taking place. In this case, electrons are drawn from the oxide which intensifies the charge in conduction band of the ferrite and hence increases the

conductivity. The difference in the sensing response to different vapours might be due to the difference in adsorption pattern and reaction mechanism [35].

## 2. Density Functional Theory (DFT) Analysis

To investigate alcohol and acetone sensing behavior of NZF, the projector augmented wave (PAW) technique [36] has been adopted as implemented in Quantum Espresso's package to perform periodic density functional theory (DFT) calculations on the zinc ferrite and nickel doped zinc ferrite (001) surfaces. In the present study, zinc ferrite (001) surface is chosen since previous studies reported that this surface is stable and mostly studied **[**37-38**]**. Furthermore, Rodríguez et al within a DFT+U scheme studied the electronic properties and the stability of (001) surface and sowed that between the two terminations, one is fully Zn-terminated surface (Zn2) and the other that "exposes" O and Fe atoms which is suitable to study the sensing behavior [38]. For optimization, the convergence threshold on the total energy of $10^{-6}$ (a.u.) and the force of $10^{-3}$ (a.u.) has been set. Wavefunctions were given a kinetic energy cutoff of 100 Ry, while charge density was given a cutoff of 400 Ry. The simulation was accomplished by utilizing the approximate generalized gradient method (GGA) with Perdew-Burke-Ernzerh (PBE) [39] and the Marzari-Vanderbilt smearing technique with a smearing threshold of 0.02 and a 1×1×1 k-point mesh [40]. In this computation, the lattice parameter a=8.46 is utilized as described previously [37]. During the simulation within the GGA+U formalism exchange and correlation effects were accounted as describe in previously literature [37].

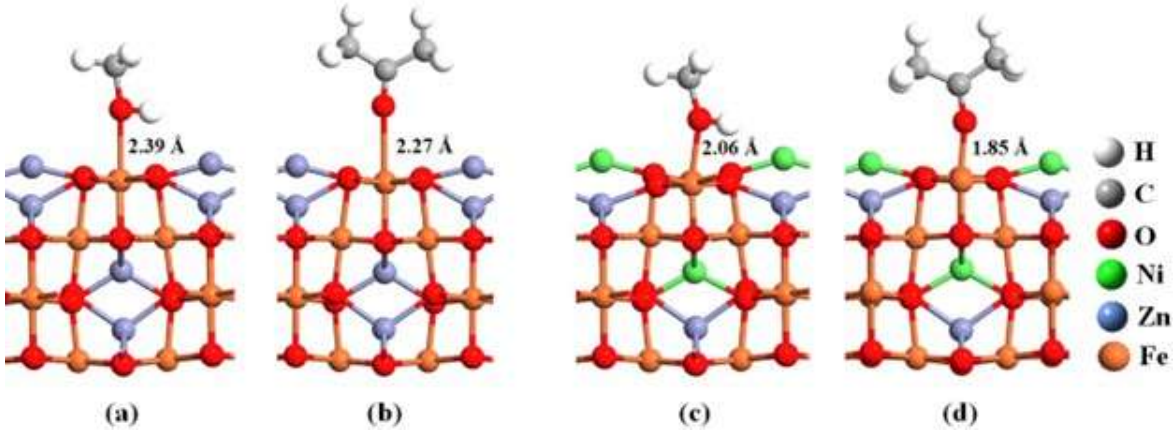


*Fig. 7. Adsorption of alcohol and acetone on the Fe-O terminated zinc ferrite (001) surface. (a) Methanol adsorbed zinc ferrite (001) surface (b) Acetone adsorbed zinc ferrite (001) surface (c) Methanol adsorbed Ni- doped zinc ferrite (001) surface (d) Acetone adsorbed Ni-doped zinc ferrite (001) surface. Red, gray, white, green and orange color represents oxygen, carbon, hydrogen, nickel and iron atoms respectively.*

To reduce the computational costs simple alcohol *viz.* methanol and acetone have been chosen for adsorption and build a unit cell of 001 surface with 5.96Å thickness. During optimization, the bottom two atomic layers were kept frozen while the remaining layers were completely relaxed during the calculations. A vacuum zone having thickness larger than 30 in the c direction to ensure no contact between the slabs has been optimized and further used for both alcohol and acetone adsorption calculations. To study the nickel doping half of the Zn atoms have been replaced with Ni atoms.

The energy minimized ground state geometries of methanol and acetone adsorbed on (001) surface is illustrated in the Fig.7. The undoped (001) surface the iron atoms showed very weak interaction with methanol and acetone as suggested by the long Fe-O bond distances of 2.39 Å and 2.57 Å respectively. With nickel doped (001) surface iron atom strongly interacts with methanol and acetone yielding very short Fe-O bonds of 2.06 Å and 1.85 Å respectively. The higher adsorption due to the presence of nickel doping can be explained by the electron pulling effect of Ni atoms which thereby increase the sensing behavior against alcohol and acetone.

In order to address how doping affect the overall electronic distribution of the zinc ferrite (001) surface, the electron localization function (ELF) is analysed as shown in the Fig. 8. The ELF study revealed that nickel doping slightly decreases the electron density on the surface and thereby accelerates the absorption of acetone and methanol.

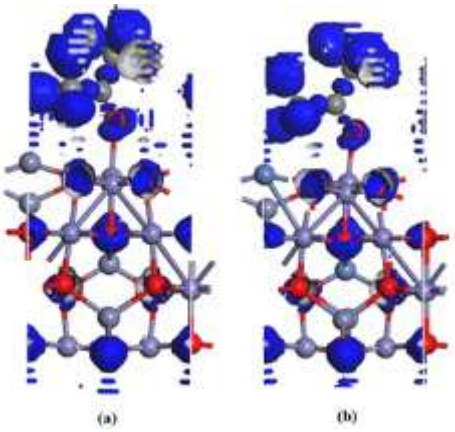


*Fig. 8. Electron localization function (ELF) of Acetone adsorbed (a) Undoped and (b) Ni-doped zinc ferrite (001) surface.*

## IV. CONCLUSION

When NZF sensors are exposed to the saturated alcohol vapours, electrical resistance is shown to vary strongly with a wide variety of response magnitudes with time showing n type conductivity. It is seen that bulk density decreases and the porosity increases progressively with increase in nickel proportion within the ferrite. This confirms that increased proportion of nickel in NZF results in dedensification of the prepared nanomaterial and consequently the sensing response increased many fold. In addition, the DFT calculation also support the pulling effect of Ni atoms in NZF nanoparticles which consequently increases the sensing properties of the prepared NZF nanomaterials. Furthermore, the ELF study backed the accelerated adsorption capacity of nickel doped nanoferrites due to slight decrease of electron density on the surface. Hence, high sensitivity of 89% and quick response towards ethanol vapour at room temperature indicating NZF1 as an excellent material in the manufacture sector of alcohol vapour detector, or electronic nose.

## ACKNOWLEDGEMENTS

Authors are thankful to The Neotia University, Department of Physics, Jadavpur University, Department of Chemistry, Malda College, Kalyani University, University of Gour Banga and Department of Botany, University of Gour Banga for providing laboratory and characterization facilities.

## FUNDING DECLARATION

This research did not receive any specific grant from funding agencies in the public, commercial, or not-for-profit sectors.

## DATA AVAILABILITY

All data generated or analysed during the study are included in the published article.

## REFERENCES

[1] Padmanathan Karthick Kannan., Ramiah Saraswathi., 2014. Impedimetric detection of alcohol vapours using nanostructured zinc ferrite. Talanta 129, 545–551.

[2] M. Ahsan, M.Z. Ahmad, T. Tesfamichael, J. Bell, W. Wlodarski, N. Motta, Low temperature response of nanostructured tungsten oxide thin films toward hydrogen and ethanol., 2012. Sensors and Actuators B 173, 789–796.

[3] F. Rumiche, H.H. Wang, J.E. Indacochea, 2012. Development of a fast response/high-sensitivity double wall carbon nanotube nanostructured hydrogen sensor, Sensors and Actuators B 163, 97–106.

[4] N. Hu, Z. Yang, Y. Wang, L. Zhang, Y. Wang, X. Huang, H. Wei, L. Wei, Y. Zhang, 2014. Ultrafast and sensitive room temperature $NH_3$ gas sensors based on chemically reduced graphene oxide. Nanotechnology 25. 025502.

[5] C. Wei, L. Dai, A. Roy, T.B. Tolle, 2006. The Chemistry of Nanostructured Materials, Journal of American Chemical Society, 2, 128, 1412–1413.

[6] M. Parmar, C. Balamurugan, D.W. Lee, PANI and Graphene/PANI Nanocomposite Films, Comparative Toluene Gas Sensing Behavior. 2013 Sensors 13, 16611–16624.

[7] H.C. Chiu, C.S. Yeh, 2007. Hydrothermal Synthesis of $SnO_2$ Nanoparticles and Their Gas-sensing of Alcohol. Journal of Physical Chemistry. *C* 111, 7256–7259.

[8] Y.J. Chen, C.L. Zhu, G. Xiao, 2008. Ethanol sensing characterization of ambient temperature sonochemically synthesized ZnO nanotubes. Sensors and Actuators B 129, 639–642.

[9] L. Wang, T. Fei, Z. Lou, T. Zhang, 2011. Three-Dimensional Hierarchical Flowerlike α-$Fe_2O_3$ Nanostructures: Synthesis and Ethanol Sensing Properties, ACS Applied Materials and Interfaces 3, 4689–4694.

[10] D. Chen, X. Hou, H. Wen, Y. Wang, H. Wang, X. Li, R. Zhang, H. Lu, H. Xu, S. Guan, J. Sun, L. Gao, 2010. The enhanced alcohol-sensing response of ultrathin $WO_3$ nanoplates, Nanotechnology 21, 035501.

[11] N. Coppede, M. Villani, R. Mosca, S. Iannotta, A. Zappettini, D. Calestani, 2013 Low Temperature Sensing Properties of a Nano Hybrid Material Based on ZnO Nanotetrapods and Titanyl Phthalocyanine. Sensors 13, 3445–3453.

[12] A.B. Gadkari, T.J. Shinde, P.N. Vasambekar, 2011 Ferrite Gas Sensors, IEEE Sensors Journal 11, 849–861.

[13] H Basti, A Hanini, M Levy, L Ben Tahar, F Herbst, L S Smiri, K Kacem, J Gavard, C Wilhelm, F Gazeau, Size tuned polyol made $Zn_{0.9}M_{0.1}Fe_2O_4$ (M = Mn, Co, Ni) ferrite nanoparticles as potential heating agents for magnetic hyperthermia: from synthesis control to toxicity survey, 2014, Materials Research Express, 1, No. 4.

[14] N. Rezlescu, E. Rezlescu, F. Tudorache, P. D. Popa. 2009. Gas sensing properties of porous Cu-, Cd and Zn- ferrites, Romanian Reports in Physics 61, No. 2, 223–234.

[15] N. S. Chen, X. J. Yang, E. S. Liu, and J. L. Huang, 2000. Reducing gas sensing properties of ferrite compounds

$MFe_2O_4$ (M = Cu, Zn, Cd and Mg), Sensors and Actuators B, 66, 1–3, 178–180.

[16] A. Sutka, J. Zavickis, G. Mezinskis, D. Jakovlevs, J. Barloti, 2013. Ethanol monitoring by $ZnFe_2O_4$ thin film obtained by spray pyrolysis, Sensors and Actuators B 176, 330–334.

[17] S.L. Darshane, R.G. Deshmukh, S.S. Suryavanshi, I.S. Mulla, 2008. Gas-Sensing Properties of Zinc Ferrite Nanoparticles Synthesized by the Molten-Salt Route, Journal of American Ceramic Society 91, 2724–2726.

[18] Y. Cao, D. Jia, P. Hu, R. Wang, 2013. One step room temperature solid phase synthesis of $ZnFe_2O_4$ nanomaterials and its excellent gas-sensing property, Ceramics International 39, 2989–2994.

[19] R. Godbole, P. Rao and S. Bhagwat, 2017, Magnesium ferrite nanoparticles: a rapid gas sensor for alcohol, Materials Research Express, 4, No. 2.

[20] A. Sutka, K. A. Grossa, 2016. Spinel ferrite oxide semiconductor gas sensors, Sensors and Actuators B 222, 95–105.

[21] N Rezlescu, E Rezlescu, 1993. The influence of Fe substitutions by R ions in a $Ni_{0.7}Zn_{0.3}Fe_2O_4$, Solid State Communications 88, 2, 139-141.

[22] M.A.M. Smeets, C. Maute, P.H. Dalton, 2002. Acute Sensory Irritation from Exposure to Isopropanol (2-Propanol) at TLV in Workers and Controls: Objective versus Subjective Effects. Annals of Occupational Hygiene 46, 359–373.

[23] C.Mukherjee, R.Mondal, S.Dey, S. Kumar and J. Das, 2017. Nanocrystalline CopperNickelZinc Ferrite: Efficient Sensing Materials for Ethanol and Acetone at Room Temperature, IEEE Sensors Journal, 17, 9, 2662-2669.

[24] A. Sutkaa, G. Mezinskisa, A. Lusisb, M. Stingaciuc. 2012. Gas sensing properties of Zn-doped p-type nickel ferrite, Sensors and Actuators B 171– 172, 354– 360

[25] I.H. Gul, F. Amin, A.Z. Abbasi, M. Anis-ur-Rehman, A. Maqsood, 2007. Physical and magnetic characterization of co-precipitated nanosize Co–Ni ferrites, Scripta Mater 56, 497–500.

[26] J.Y. Patil, M.S. Khandekar, I.S. Mulla, S.S. Suryavanshi, 2012. Combustion synthesis of magnesium ferrite as liquid petroleum gas (LPG) sensor: Effect of sintering temperature, Current Applied Physics 12, 319–324.

[27] A.S. Fawzi, A.D. Sheikh, V.L. Mathe, 2010. Structural, dielectric properties and AC conductivity of $Ni_x Zn_{(1-x)}Fe_2O_4$ spinel ferrites, Journal of Alloys and Compounds 502, 231–237.

[28] K. Rama Krishna, K. Vijaya Kumar and Dachepalli Ravinder, 2012. Structural and electrical conductivity studies in Ni-Zn Ferrite, Advances in Materials Physics and Chemistry 2, 185-191.

[29] G. Korotcenkov, 2007. Metal oxides for solid-state gas sensors: What determines our choice? Materials Science and Engineering: B 139, 1–23.

[30] R.B. Kamble, V.L. Mathe. 2008. Nanocrystalline nickel ferrite thick film as an efficient gas sensor at room temperature, Sensors and Actuators B 131, 205–209.

[31] R. Srivastava & B.C. Yadav, 2014. Nanostructured $ZnFe_2O_4$ thick film as room temperature liquefied petroleum gas sensor, Journal of Experimental Nanoscience 10, 1-15.

[32] X.Zhou, Q.Xue, H.Chen and C.Liu, 2010. Current–voltage characteristics and ethanol gas sensing properties of ZnO thin film/Si heterojunction at room temperature, Physica E 42, 2021-2025.

[33] A. B. Gadkari, T. J. Shinde, and P. N. Vasambekar, 2011. Ferrite Gas Sensors, IEEE Sensors journal 11, 849-861.

[34] Z.P. Sun, L. Liu, D.Z. Jia, W.Y. Pan, 2007. Simple synthesis of $CuFe_2O_4$ nanoparticles as gas-sensing materials, Sensors and Actuators B 125, 144-148.

[35] V. Lantto and P. Romppainen, 1987. Electrical studies on the reactions of CO with different oxygen species on $SnO_2$ surfaces, Surface Science 192, 243–264.

[36] P. Giannozzi, S. Baroni, N. Bonini, M. Calandra, R. Car, C. Cavazzoni, D. Ceresoli, G. L. Chiarotti, M. Cococcioni, I. Dabo, A. Dal Corso, S. de Gironcoli, S. Fabris, G. Fratesi, R. Gebauer, U. Gerstmann, C. Gougoussis, A. Kokalj, M. Lazzeri, L. Martin-Samos, N. Marzari, F. Mauri, R. Mazzarello, S. Paolini, A. Pasquarello, L. Paulatto, C. Sbraccia, S. Scandolo, G. Sclauzero, A. P. Seitsonen, A. Smogunov, P. Umari and R. M. Wentzcovitch, *J. Phys. Condens. Matter*, 2009, **21**, 395502.

[37] Rodríguez, KL Salcedo, JJ Melo Quintero, HH Medina Chanduví, AV Gil Rebaza, Ricardo Faccio, Waheed A. Adeagbo, Wolfram Hergert, CE Rodríguez Torres, and Leonardo Antonio Errico. "Ab-initio approach to the stability and the structural, electronic and magnetic properties of the (001) Znfe2O4 surface terminations." Applied Surface Science 499 (2020): 143859.

[38] Rezende, A.F.D., Oliveira, M.C.D., Ribeiro, R.A.P., Mesquita, W.D., Marques, J.D.J., Magalhães, N.F.D.S., Lemes, J.H.V., Longo, E. and Gurgel, M.F.D.C., 2022. DFT Calculations for Structural, Electronic, and Magnetic Properties of ZnFe 2 O 4 Spinel Oxide: The Role of Exchange-Correlation Functional. *Materials Research*, *25*.

[39] J. P. Perdew, K. Burke and M. Ernzerhof, *Phys. Rev. Lett.*, 1996, **77**, 3865–3868.

[40] N. Marzari, D. Vanderbilt, A. De Vita and M. C. Payne, *Phys. Rev. Lett.*, 1999, 82, 3296–3299.

## AUTHOR CONTRIBUTIONS

**Chandra Mukherjee:** Conceptualization; data curation; formal analysis; investigation; methodology; validation; visualization; roles/writing—original draft.

**Subhankar Choudhury:** Software; validation; methodology.

**Nabajyoti Baildya:** Software; investigation.

**Narendra Nath Ghosh:** Data curation; visualization; roles/writing—original draft.

**Debabrata Misra:** Resources; validation; writing—review and editing.

**J. Das:** Conceptualization; formal analysis; funding acquisition; resources; supervision; validation; visualization; writing—review and editing.